An antibacterial and anti-oxidative hydrogel dressing for promoting diabetic wound healing and real-time monitoring wound pH conditions with a NIR fluorescent imaging system

Yuange Zong ‡[a], Beige Zong ‡[c], Ruyan Zha[a], Yi Zhang[a], Xianghong Li[a], Yanying Wang [a], Huaifang Fang [a,], Wing-Leung Wong [b,*] and Chunya Li [a,*]*

[a] Key Laboratory of Catalysis and Energy Materials Chemistry of Ministry of Education & Key Laboratory of Analytical Chemistry of the State Ethnic Affairs Commission, College of Chemistry and Materials Science, South-Central Minzu University, Wuhan 430074, China.

[b] State Key Laboratory of Chemical Biology and Drug Discovery, Department of Applied Biology and Chemical Technology, The Hong Kong Polytechnic University, Hung Hom, Kowloon, Hong Kong SAR, China.

[c] Chongqing Emergency Medical Center, Chongqing University Central Hospital, School of Medicine, Chongqing University, Chongqing, China

‡ The first two authors contributed equally to this work.

* Corresponding author

E-mail (H.F. Fang): hffang@mail.scuec.edu.cn

E-mail (W.L. Wong): wing.leung.wong@polyu.edu.hk

E-mail (C. Li): lichychem@mail.scuec.edu.cn

This article has been accepted for publication and undergone full peer review but has not been through the copyediting, typesetting, pagination and proofreading process, which may lead to differences between this version and the Version of Record. Please cite this article as doi: 10.1002/adhm.202300431.

Keywords: Diabetic Wound, Injectable, Antibacterial, Antioxidant, Real-Time Monitoring

Abstract

The design and synthesis of multi-functional chitosan hydrogels based on polymerized ionic liquid and a near-infrared (NIR) fluorescent probe (PIL-CS) is a promising strategy, which not only prevents the transition from acute to chronic wounds, but also provides prompt measures regarding microenvironmental alterations in chronic wounds. PIL-CS hydrogel can real-time visualize wound pH through *in vivo* NIR fluorescent imaging and also feature the pH-responsive sustained drug release, such as antioxidant, to eliminate reactive oxygen species (ROS) and to boost diabetic wound healing. PIL-CS hydrogel is specific, sensitive, stable and reversible in response to pH changes at the wound site. It, therefore, enables real-time monitoring for a dynamic pH change in the microenvironment of irregular wounds. PIL-CS hydrogel was also designed to possess many merits including high water containment and swelling rate, good biocompatibility, electrical conductivity, antifreeze, tissue adhesion, hemostatic performance, and efficient antibacterial activity against MRSA. *In vivo* studies showed that PIL-CS hydrogel provided fast diabetic wound healing support, promoted VEGF production, and reduced ROS and TNF-α generation. The results support that the hydrogels coupled with NIR fluorescent probes could be an excellent diabetic wound dressing for enhancing and real-time monitoring skin restoration and regeneration.

1. Introduction

Skin is the largest organ of the physique and is critically important in resisting the invasion of foreign bacteria and maintaining the body's metabolism.[1] Acute and chronic wounds caused by injury or diabetes disrupt the integrity of skins and result in either open or deep and irregular wounds that are susceptible to infection and inflammation. A lack of effective detection and care for wounds leads to the conversion of acute wounds into chronic ones.[2] Diabetic wounds, as one of the representative chronic wounds, not only incur additional long-term treatment costs but also lead to amputation or even death if care failed.[3] Diabetic wounds are often associated with serious bacterial infection and inflammation, which reduce greatly the formation and deposition of extracellular matrix (ECM).[4] In addition, a sharp surge of large amounts of reactive oxygen species (ROS) induces an unbalance of pro- and anti-inflammatory cells/factors, which impede chronic scar tissue regeneration.[5] Real-time monitoring wound healing process thus prevents bacterial infection and inflammation, and also provides help for chronic wound management and treatments.

Real-time monitoring of wound infection and alterations in the microenvironment of diabetic wounds is able to provide essential information to healthcare providers regarding wound healing. This function may facilitate a more efficient and personalized promotion of wound healing.[6] It is reported that normal skin has an acidic environment and the pH is usually in the range of 4 – 6 which makes the skin resistant to outside injury. Once skin damage has occurred, it results in an acute wound. The pH rises slightly as it undergoes a rapid repair process (hemostasis and inflammation) and keep in an acidic environment as the wound site tissues add and remodel.[1] However, due to a number of factors influenced by infection, inflammation and diabetes, acute wounds are highly susceptible to be chronic and that results in a significant increase in pH in an alkaline environment (pH 7 - 8).[7] The wound area has an alkaline environment that is more suitable for bacterial growth. Bacterial infection may cause a vicious cycle of inflammation that may worsen the wound conditions and even

lead to tissue necrosis and amputation. Therefore, real-time monitoring of pH at the wound may provide a reliable reference for wound caring. Electrochemical sensors[8] and fixed dye dressings[9] have been commonly developed to monitor the pH status of wounds, but there are still drawbacks such as unstable performance and high toxicity due to easy contamination, which limit the clinical application. Fluorescent probes are designed to connect fluorophores and recognition units to detect objects, and are the most commonly used materials for constructing fluorescent detectors. In order to achieve high stability, specificity, low toxicity, reversibility and high sensitivity for real-time monitoring of pH. We designed and synthesized a specific pH-responsive near-infrared (NIR) fluorescent probe, CyO, for real-time monitoring of pH changes at wounds. The probe has good water solubility and is easily grafted onto the hydrogel mesh structure via amide bonds to form NIR fluorescent PIL-CS hydrogels. In addition, NIR fluorescent probes have been widely studied for in vivo detection in recent years.[10] The hydrogel integrated with CyO is thus considered an excellent tool for monitoring wound pH microenvironment and promoting diabetic wounds healing in real-time.

As a diabetic wound dressing, it could be more attractive to offer additional functions such as antioxidant and ROS scavenging ability by stimulating drug release through intelligent response.[11] Metformin hydrochloride (MH), a widely used clinical drug for type II diabetes, may be useful in increasing insulin sensitivity of peripheral local cells, increasing re-epithelialization of endothelial cells, and diminishing the accumulation of metallo-matrix protease (MMP) at chronic wound sites.[12] To achieve this, MH was grafted onto polyionic liquids with aldehyde groups (PIL-CHO) via Schiff base structures. Thus, transient acidic changes in the wound microenvironment caused by inflammation could dissociate the Schiff base structure. A better MH release may facilitate diabetic wound healing.[13] Dihydrocaffeic acid (DA), a biocompatible antioxidant drug, after being grafted into the chitosan backbone through the amide structure, can offer tissue adhesion and antioxidant properties to

hydrogels.[14] On the other hand, L-arginine (LAG), a cationic amino acid capable of increasing angiogenesis and promoting insulin secretion, may maintain its dominance when it is grafted onto the chitosan backbone.[12]

Proper wound care usually includes pressure to stop bleeding, clean debridement, and dressing application. Compared to marketed dressings (foams, films and alginate excipients), hydrogel, a three-dimensional structured polymer using water as a medium, has a similar moist environment to the skin physiology, which is more conducive to wound healing.[1] It can also be readily functionalized to fit the special need of diabetic wounds by modifying the polymer chain of the hydrogel. Bacterial infection is also a critical concern for chronic wound healing in diabetic individuals.[15] The treatment often requires antibiotics, nanometals or releasable silver as a bactericidal prevention and treatment; however, the treatment may cause bacteria to be drug-resistant (e.g. MRSA) [16] and have toxic side effects.[17] Both chitosan (CS) and cationic poly-ionic liquid (PIL-CHO) are typical non-releasable antimicrobial materials with positively charged functional groups that interact with the anionic phosphate group of bacterial cell walls through electrostatic interactions. In addition, the introduction of hydrophobic groups may disrupt bacterial cell membranes and thereby kill bacteria by lysis.[18]

In the present study, we developed a PIL-CS hydrogel for real-time monitoring of the wound pH and facilitating diabetic wound healing (**Figure 1**). The structure of PIL-CS hydrogel is composed of a CS backbone grafted with DA and LAG, and a PIL-CHO backbone with a Schiff-base structure with MH. To provide the real-time monitoring function, a NIR fluorescent probe CyO was integrated into the network structure of the hydrogel through the formation of amide bonds. The functionalized hydrogel could achieve a highly sensitive, specific and reversible response to pH changes in a range of 4.5 - 8.8 at the wound microenvironment. From the results obtained with a NIR fluorescence in the vivo imaging system, it showed a dependence of fluorescence intensity on pH and a good linear

relationship was obtained. Therefore, the dynamic pH of the wound microenvironment could be quickly monitored in real-time by measuring the changes in fluorescence intensity. The PIL-CS hydrogel also showed good antioxidant properties and antibacterial activity against *E. coli*, *S. aureus*, *B. subtilis* and *MRSA*. Moreover, it could endure the release of pH-responsive drugs and promote cell migration. It also could fight inflammation and promote angiogenesis. These merits of PIL-CS hydrogel rendered many potential applications. Particularly, it could be an attractive promoter of wound healing and real-time monitoring for the prevention of wound inflammation.

15

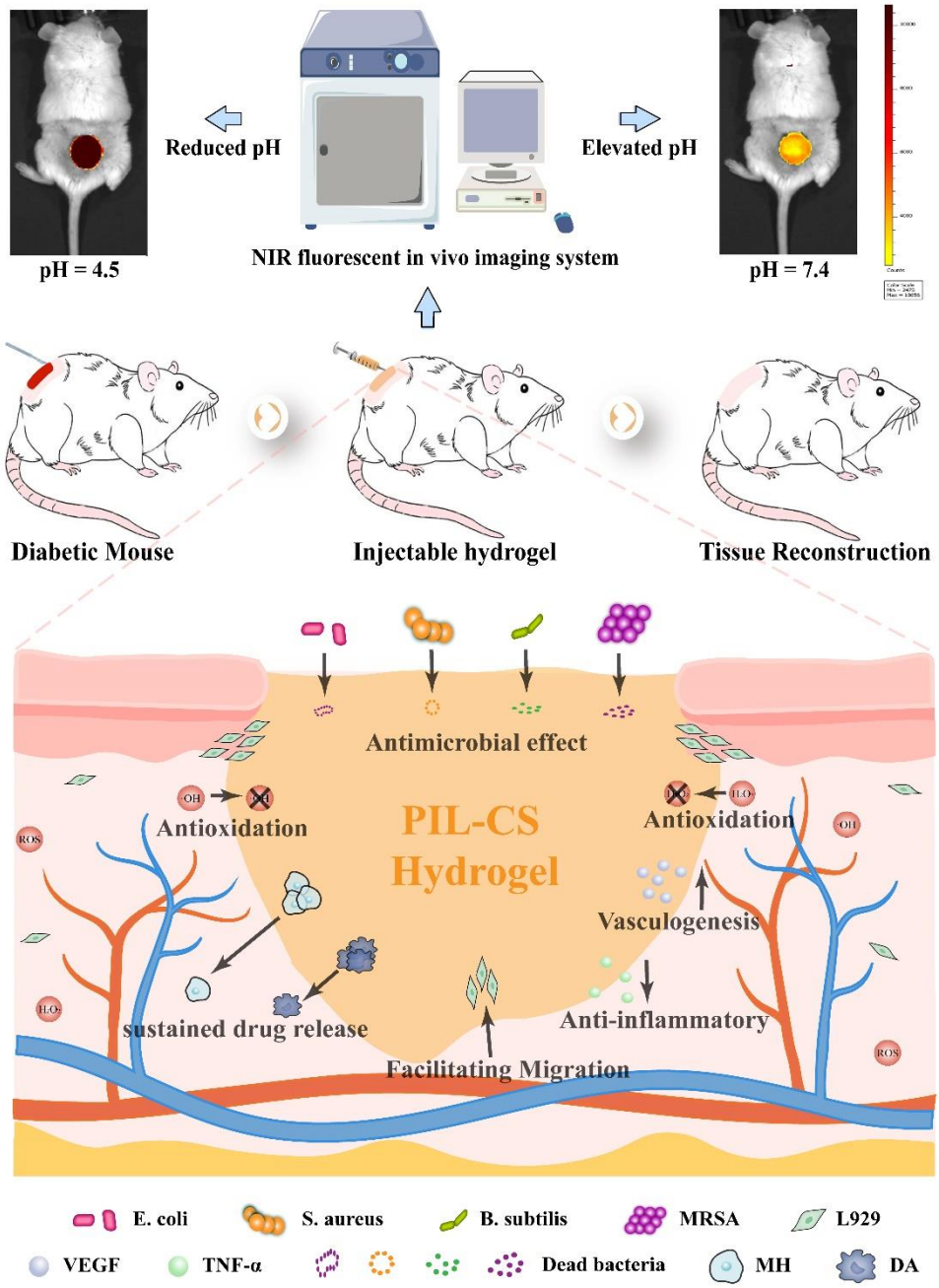

Figure 1. Real-time imaging schematic of NIR fluorescent hydrogel PIL-CS on in vivo diabetic mice and effective facilitation of diabetic wound healing through effective

antimicrobial properties, antioxidant properties, sustained drug release, promotion of cell migration, anti-inflammatory and promotion of angiogenesis.

2. Results and Discussion

2.1 The capability of a NIR fluorescent probe (CyO) for pH measurement

To estimate the performance of the NIR fluorescent probe, CyO, for the detection of pH conditions, a series of fluorescence tests were carried out. First, the absorption and emission spectra of CyO in a methanol-buffer solution were measured. As shown in **Figure 2A**, an absorption peak found at 820 nm confirmed the NIR property of CyO. The long wavelength excitation and emission can benefit biological applications such as in vivo imaging. Next, the magnitude of the fluorescence was recorded in methanol solution with various pH conditions (pH 2.0 - 9.0) (**Figure S7A**). It was found that the fluorescence intensity of the probe was the highest at pH 4.5 and the fluorescence intensity shows no observable changes at pH 8.0-9.0. In addition, when the pH is less than 4.5, the fluorescence signal increased. It may be caused by the disruption of the large π conjugate system of the probe.[19] For the pH ranging from 4.5 to 7.4, the emission signal also decreased gradually as shown in **Figure 2B**. It may be due to the expansion of the π conjugate system. A linear relationship between the fluorescence intensity of the probe and the corresponding pH was obtained (**Figure 2C**).

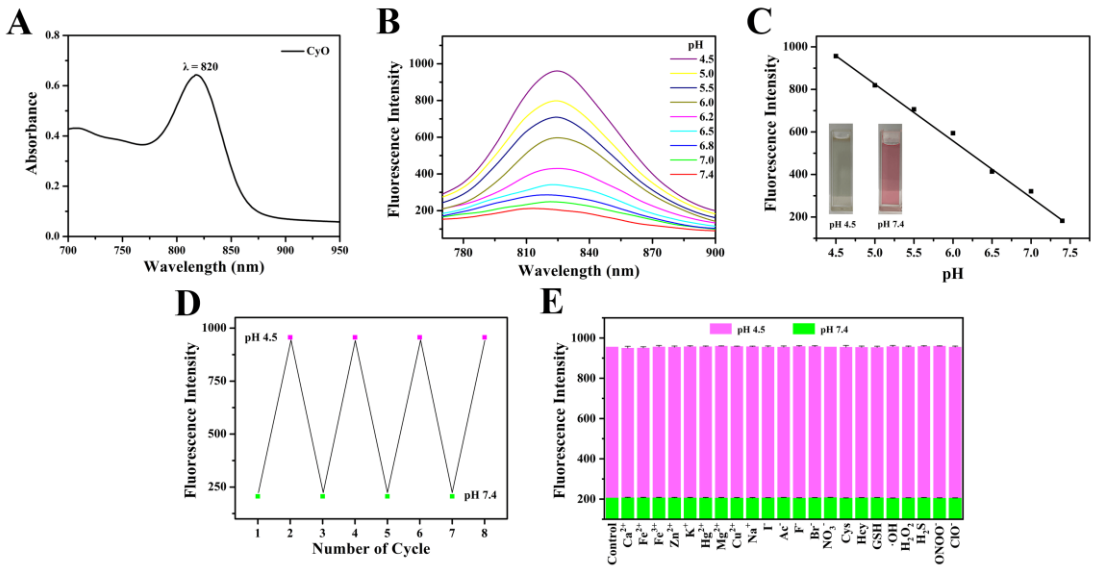

Figure 2. Characteristics of NIR fluorescent probes. A) The absorption spectrum of the NIR fluorescent probe CyO (10 μM) in methanol solution; B) Fluorescence emission spectra of CyO (10 μM) after multiple pH adjustments (pH 4.5 - 7.4) in methanol. C) Linear correlation between the fluorescence strength of the probe and pH values. D) Fluorescence intensity of CyO (10 μM) with repeated switching of pH (4.5/7.4). λex/λem = 725/820 nm. E) Fluorescence reaction of CyO (10 μM) to various analytes (1 mM) in methanolic solutions at pH 4.5 and 7.4, separately.

The reversibility of CyO is also demonstrated by repeatedly adjusting the pH of the buffer as shown in **Figure 2D**. The results illustrate the suitability of the probe for real-time monitoring of pH changes in the microenvironment of biological samples. In addition, the fluorescence intensity of CyO was confirmed to be virtually unaffected by temporal changes as indicated by the steady fluorescence intensity measured at pH 4.5-7.4 for 30 days (**Figure S7B**). The results indicate that CyO has excellent stability. As shown in **Figure 2E**, the specificity of CyO for pH measurement was determined by adding different analytes to interfere with the probe at pH 4.5-7.4. It was found that common analytes include cations

(Ca^{2+}, Fe^{2+}, Fe^{3+}, Zn^{2+}, K^{+}, Hg^{2+}, Mg^{2+}, Cu^{2+}, Na^{+}), anions (I^{-}, Ac^{-}, F^{-}, Br^{-}, NO^{3-}), and ROS ($\cdot OH$, H_2O_2, H_2S, $ONOO^{-}$, ClO^{-}) show no interference effects to the probe at pH 4.5-7.4.

The biosafety of hydrogel dressings is also a critical factor of consideration for biological applications. To assess the cytocompatibility of CyO at different concentrations (5, 10, 15 and 20 μM), the probe was co-cultured with L929 cells to evaluate its toxicity. Double staining of live/dead cells with Calcein-AM/PI showed (**Figure S7C**) that almost no dead cells were observed after 2 days. CCK-8 results showed (**Figure S7D**) that the cell viability remained close to 96% after 3 days. Both results indicate that CyO has high biocompatibility.

2.2 Characterization of NIR fluorescent hydrogels

The raw materials for the synthesis of PIL-CS hydrogels: NIR fluorescent pH probe CyO (Figure S1), PIL-CHO (Figure S3) and CS-DA-LAG (Figure S5), respectively, were prepared according to the support infographic, and the successful preparation of CyO (Figure S2) and PIL-CHO (Figure S4) was verified based on ^{1}H NMR. The FTIR spectrograms and ^{1}H NMR hydrogen spectra of CS-LAG, CS-DA and CS-DA-LAG were analyzed to compare Figure S6 to confirm the successful grafting of DA and LAG. the peak of CS-DA at 2.61 ppm was derived from the hydrogen attached to the methylene group of the benzene ring, which proved the successful grafting of DA. CS-DA-LAG was further prepared by grafting LAG onto CS-DA polymer, which not only prevented the oxidation of catechol but also enhanced its tissue adhesion. The peaks of CS-DA-LAG at 4.17, 3.15, 2.47 and 2.32 ppm were consistent with CS-LAG and different from CS-DA, confirming the successful grafting of LAG.

PIL-CS hydrogel is a liquid at room temperature (**Figure 3A**). When the temperature rises to about 37 °C, PIL-CS hydrogel changes immediately its physical state from sol to gel.

Moreover, when a hydroxylamine solution is added to the hydrogel, the gel state gradually changes back to the sol-gel state. This is because hydroxylamine competes with amino groups and breaks the Schiff base and amide bonds in PIL-CS hydrogels. The dynamic polymer network is thus disrupted. The single polymeric chain in the hydrogels also forms dynamic networks through Schiff base and amide bonds. The energy storage modulus (G') and energy dissipation modulus (G") of the PIL-CS hydrogel with increasing temperature are monitored by dynamic rheometry as shown in **Figure 3B**. G' is less than G" when the temperature is below 37 °C. This may imply that the sample has low viscosity and is an injectable solute. When the modulus increases with temperature, an increasing trend of G' is observed and the magnitude increased is greater than G". The intersection of G' and G" is usually considered to be the transformation temperature at which the sol becomes a gel.[20] At room temperature, PIL-CS hydrogel can be easily extruded from the syringe and letters can be drawn without any drag with the syringe as shown in **Figure 3C** and **supporting video S1**. This could be attributed to the Schiff base structure as dynamic chemical bonding in a large proportion of the PIL-CS hydrogel structure. Therefore, PIL-CS hydrogel is excellent in injectability and can adapt to any irregular wound and offer a large contact area at the wound. Therefore, PIL-CS hydrogel may promote wound healing. In **Figure 3D**, the increase in G' and G" of the PIL-CS hydrogel with time is also observed. The intersection of G' and G" was found to be about 330 s, which was the expected gelation time of PIL-CS hydrogel. The PIL-CS hydrogel was cut and reassembled to observe the self-healing ability (**Figure 3E**). The sign of cut is observed at 0 h. A part of the cut-area is disappeared at 1 h. Some self-healing cross-linked networks are formed again at the cut position which can be observed clearly by applying a force to pull the hydrogel with forceps. The results indicate that PIL-CS hydrogel has good self-healing ability.

The PIL-CS hydrogel was prepared by controlling the content of the ionic liquid IL-CHO (0, 3, 6 and 9 wt%) by naming them PIL-CS-X (X = 1, 2, 3 and 4), respectively. As

shown in **Figure 3F**, the microstructure of the hydrogel was observed by field emission electron microscopy (SEM). The hydrogel showed a distinct 3D porous morphology and the pore size of PIL-CS-1 to PIL-CS-4 hydrogels became smaller gradually by increasing the IL-CHO content in the preparation. This is attributed to the reduction of crosslink density in the hydrogel with increasing IL-CHO content. Furthermore, the porous morphology provides support for gas exchange at the wound site. The chemical architecture of PIL-CS hydrogels was characterized by Fourier transform infrared spectroscopy (FT-IR) (**Figure 3G**). The feature peaks at 1463 and 1689 cm^{-1} were assigned as (-C=N-) in the Schiff base bond and (-C-N-) in the amide bond. The characteristic peaks at 2996 and 3417 cm^{-1} were assigned to (-CHO) in the polyionic liquid and (-OH) in the modified CS. In addition, the characteristic peaks of (-C=N-), (-C-N-) and (-CHO) tend to increase progressively. This is attributed to the increase in chemical cross-linking by increasing IL-CHO content in PIL-CS hydrogels. However, the (-OH) peak is almost constant because the content of modified CS in PIL-CS hydrogels is the same. In addition, the zeta potential of the PIL-CS-4 hydrogel was 50.13 mV, which implies a positive point in the hydrogel band (**Figure S8A**). This is attributed to the cationic polyionic liquids (PILs) formed in the hydrogel structure. The cations of PILs can destroy the bacterial cell wall via electrostatic interactions with the anionic phosphate groups of bacterial cell walls. Consequently, bacteria are killed by lysis.[21] BSA under physiological conditions is negatively charged and is adsorbed easily by positively charged hydrogels through electrostatic interactions.[22] When the water content is absorbed by PIL-CS hydrogels at around 70% (**Figure S8B**), the swelling rate is about 283 - 495% (**Figure S8C**). The BSA adsorption was about 281.25 - 325 mg (**Figure S8D**). PIL-CS hydrogel thus provides a moistened environment for wounds and adsorbs metabolic waste from cells. These properties can provide a good healing environment for wounds.

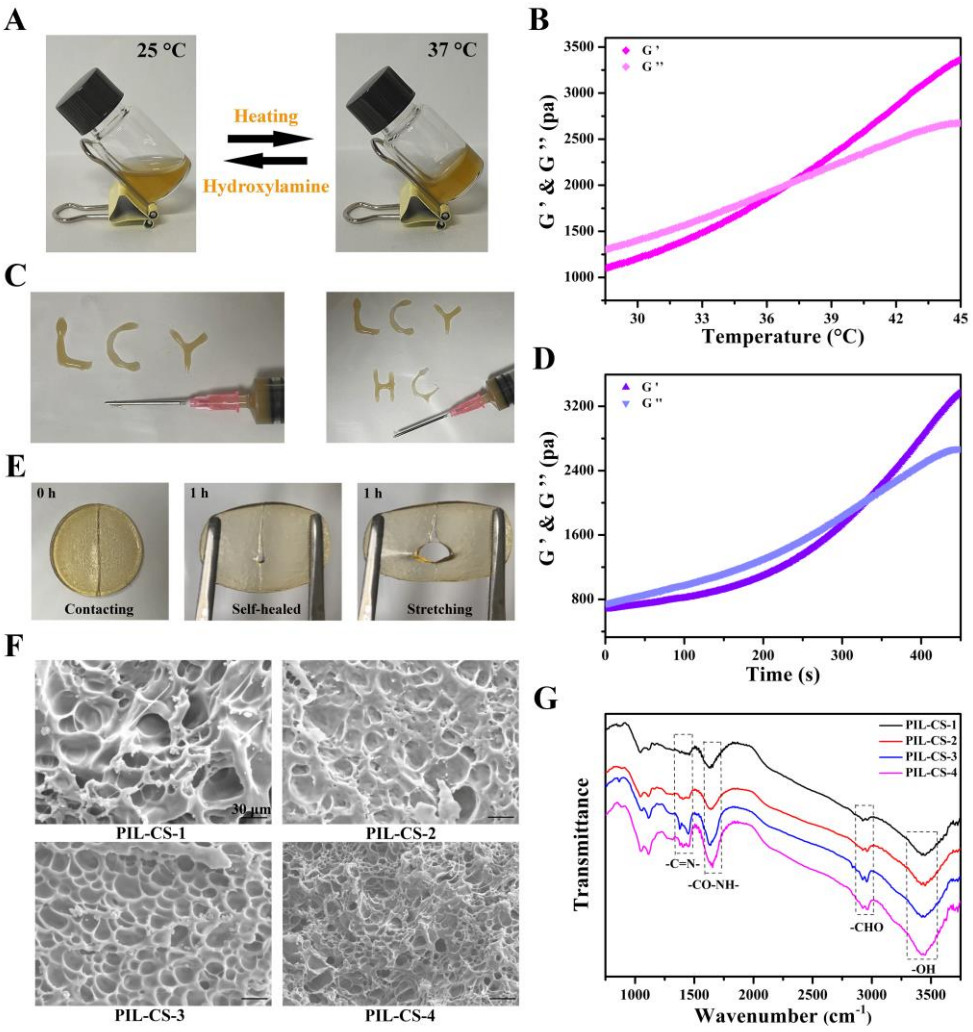

Figure 3. Preparation and physical-chemical structural characterization of near-infrared fluorescent responsive PIL-CS-X (X=1, 2, 3, 4). A) Photographs for the sol-gel transition of PIL-CS-4 hydrogel; B) The dependence of the energy storage modulus (G') and energy dissipation modulus (G") of the PIL-CS-4 hydrogel on temperature; C) Injectability of PIL-CS-4 hydrogel through a syringe; D) The dependence of the energy storage modulus (G') and energy dissipation modulus (G") of the PIL-CS-4 hydrogel on temperature time; E) Self-healing behavior of PIL-CS-4 hydrogels versus time; F) Representative SEM images of PIL-CS-X hydrogels; G) FTIR spectra of PIL-CS-X hydrogels.

2.3 Physical properties and characteristics of the NIR fluorescent hydrogels

For practical applications, the PIL-CS hydrogel needs to have a good mechanical property that meets the requirement of being a wound dressing. The tensile and compressive stresses of PIL-CS hydrogels were tested. In general, the PIL-CS hydrogel exhibited good tensile and compressive properties, which were stretching to 150 % - 254 % before gradually breaking. In addition to a gradual increase in maximum stress from 0.32 to 0.81 Mpa with an increasing crosslink density (**Figure 4A**). Due to the good mechanical property of the PIL-CS hydrogel, it does not rupture even when the compressive stress is higher than 80 %, but the maximum stress increases from 0.23 to 2.13 Mpa as the cross-link density increases (**Figure 4B**). **Supporting video S2** illustrates that the PIL-CS hydrogel adheres firmly to skin surfaces without breaking after a constant and repeated stretching test. These experiments confirmed that the increase of cross-link density could improve the mechanical property of PIL-CS hydrogels. To further quantify the adhesion of the hydrogel dressing to the skin and verify its ability to reduce tissue damage from external forces, shear lap experiments were conducted using a piece of pig skin as a model for evaluation. As shown in **Figure 4C**, the hydrogel exhibits an adhesive strength between 0.18 - 0.53 Mpa. The **supporting video S3** also demonstrates the strong adhesion of PIL-CS hydrogel to the skin. The good tissue adhesion could be a result of DA and LAG that enhance the adhesion. The good tissue or skin adhesion ability ensures the dressing is adhered closely to the wound.[9] Moreover, it is noteworthy that even though the PIL-CS hydrogel has good adhesion properties, it can be removed readily from the skin and without pulling the surrounding skin (**Figure 4D** and **supporting video S4**).

Conductive hydrogels are known to facilitate the immigration and multiplication of endothelial cells. It is thus beneficial to angiogenesis.[23] The PIL-CS hydrogel is very

conductive and can be used as a portion of the electrical circuit to illuminate a LED (**Figure 4E**). The conductivity of the hydrogels was found to increase from 0.23 to 0.76 mS cm^{-1} with increasing PIL-CHO concentration (**Figure 4F**). Tissue skins have a conductivity between 10^{-5} ~ 0.26 S m^{-1}.[24] It is reported that hydrogels with an electrical conductivity comparable to that of skin may effectively accelerate wound healing.[25] Hydrogels with anti-freeze properties can be better adapted to low temperature environments. IL-CHO is an ionic liquid and provides ions in the hydrogel system to reduce the crystallization temperature of the water.[21] As shown in **Figure S9** and **supporting video S5**, in a low-temperature environment at around -40 °C, the PIL-CS hydrogel still maintains good electrical and mechanical properties, which indicate that the material has good environmental adaptability and stability.

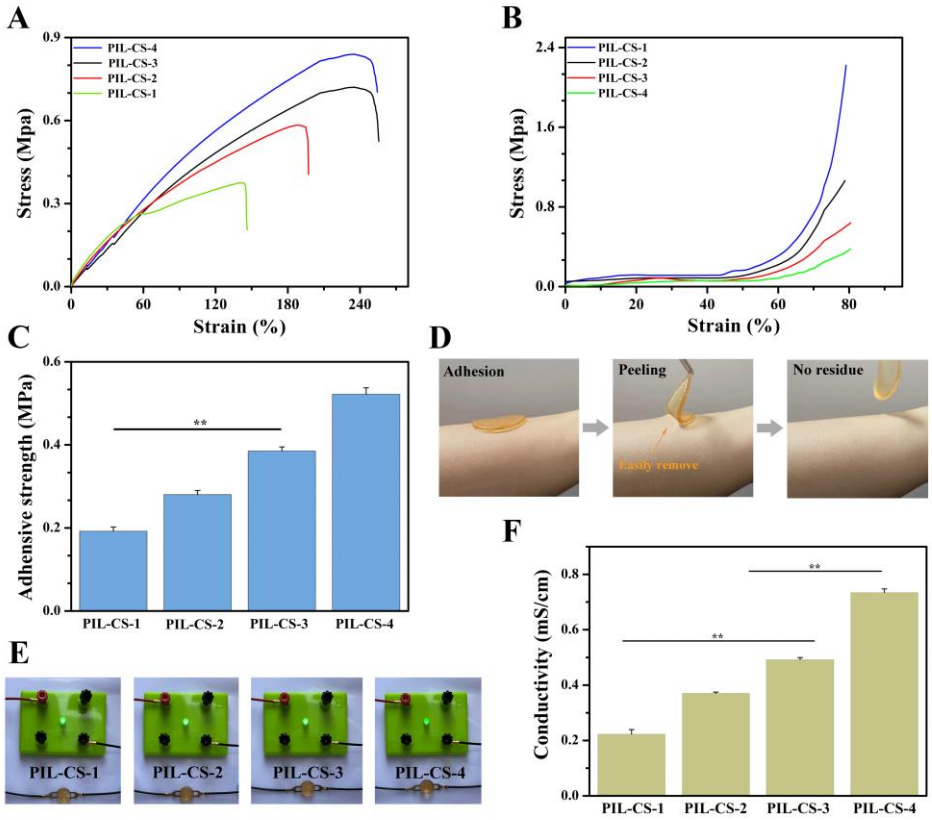

Figure 4. Multifunctional features of PIL-CS-X (X=1, 2, 3, 4) hydrogel. A) Tensile stress-strain curve of PIL-CS hydrogel under tension; B) Compressive stress-strain curve of PIL-CS hydrogel in compression; C) Adhesion properties of PIL-CS hydrogel (data are depicted as mean ± SD, $^{**}p < 0.01$, n = 3); D) Optical photographs of the PIL-CS hydrogel removal procedure; E) Optical photo of PIL-CS hydrogel being used as part of the circuit to illuminate the LED; F) Electrical conductivity of PIL-CS hydrogels (data are depicted as mean ± SD, $^{**}p < 0.01$, n = 3).

2.4 NIR fluorescent hydrogel as a carrier for pH-responsive drug releasing

Metformin hydrochloride (MH) is a commonly used drug for type 2 diabetes and has recently been shown to play a role in increasing cellular sensitivity to insulin.[4] In diabetic wounds, MH also induces cell proliferation and reduces apoptosis.[26] However, due to the low bioavailability of oral MH, it is better suited for promoting diabetic wound healing through the Schiff base structure grafting into hydrogels. Then, using the weak acid character of the wound inflammatory response may be able to disrupt the Schiff base structure and release MH at the wound site.[27] In addition, dihydrocaffeic acid (DA) exhibits good antioxidant activity and reduces ROS production. DA thus helps in the healing of chronic inflammatory wounds.[28] Under different pH conditions (5.5, 6.8 and 7.4) at 37 °C, DA is released from the media to the wound environments. PIL-CS hydrogel can be a good carrier for MH and DA. The drug can be released to pH response at the wounds. The release of MH at different pH was found almost constant. The release of MH is found to increase from pH 7.4 to 5.5, indicating that the acidic environment enhances drug release (**Figure 5A**). In a 160-hour experiment, the rate of MH release was found to be 27.34% at pH 7.4, 71.68% at pH 6.8 and 94.36% at pH 5.5. The release of MH from PIL-CS hydrogel shows an obvious pH dependence. For the case of DA, its release from PIL-CS hydrogel was found to be 61.93% at pH 7.4, 82.96% at pH 6.8 and 97.74% at pH 5.5 (**Figure 5B**).

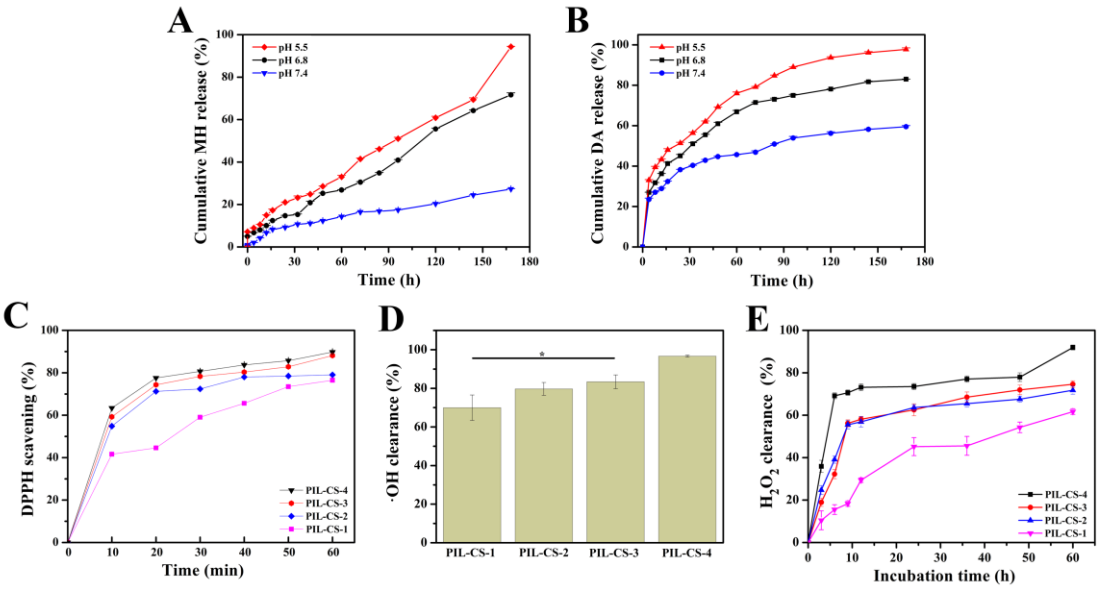

Figure 5. Drug slow release, and antioxidant and ROS scavenging properties of NIR fluorescent PIL-CS-X (X=1, 2, 3, 4). A) pH-responsive release of metformin hydrochloride. B) pH-responsive release of dihydrocaffeic acid. Comparison of the contribution of antioxidant capacity of PIL-CS hydrogels. DPPH (C), hydroxyl radical (D) and H_2O_2 (E) (data are depicted as mean ± SD, *$p < 0.05$, $n = 3$) .

In chronic wounds, the continuous inflammatory response and the dramatically increased ROS may cause a large accumulation of free radicals. Consequently, the oxidative stress is induced.[29] It is reported that wound dressings with antioxidants that have ROS scavenging abilities may significantly prevent wound infections and also promote wound healing.[30] The antioxidant capacity of PIL-CS hydrogel was measured by DPPH scavenging assay.[31] As shown in **Figure 5C**, PIL-CS hydrogels tested exhibited DPPH clearing efficiencies, which were found to be 76.35 % (PIL-CS-1), 79.84 % (PIL-CS-2), 88.75 % (PIL-CS-3) and 89.95 % (PIL-CS-4) in the removal of DPPH after 60 min, respectively. We found that PIL-CS hydrogels carried with DA and MH may have antioxidant activity due to these drugs being excellent antioxidants.[32] In addition, the catechol structure in DA can capture ROS. It thus reduces oxidative stress and may enhance chronic wound healing.

In addition, the ability of PIL-CS hydrogels to scavenge ROS was assessed by using tetramethyl benzidine (TMB) as an indicator for the ·OH radical and using $Ti(SO_4)_2$ as an indicator for H_2O_2. **Figure 5D** shows that 69.98 % (PIL-CS-1), 75.70 % (PIL-CS-2), 83.39 % (PIL-CS-3) and 96.65 % (PIL-CS-4) of ·OH are removed after co-incubation with the PIL-CS hydrogels. **Figure 5E** shows that PIL-CS hydrogels continuously remove H_2O_2 for at least 60 h.

2.5 *In vitro* antimicrobial evaluation

Diabetic wounds have high glycemic and pH characteristics and are more susceptible to bacterial infection than acute wounds. It thus causes a vicious cycle. Therefore, the ideal excipients should have excellent antibacterial activity without causing bacterial resistance.[33] The antibacterial ability of four PIL-CS hydrogels against *E. coli*, *S. aureus*, *B. subtilis* and MRSA was measured by in vitro contact culture with bacteria. As shown in **Figure 6**, the PIL-CS hydrogel produced significant inhibition circles on all four colonies. This non-release antibacterial ability of PIL was further supported by the largest inhibition circle of PIL-CS-4 hydrogel. The SEM images of live/dead bacteria inside and outside the inhibition circle also illustrate indirectly that the bactericidal mechanism of PIL-CS hydrogel is to lyse the bacteria.[21] Quantitative analysis of the area of the inhibition circle confirmed the bactericidal ability of PIL-CS hydrogel against both Gram-negative and positive bacteria and resistant MRSA, indicating that PIL-CS hydrogel has an excellent broad-spectrum antibacterial property. The SEM chart also side-by-side confirms that is mainly due to the positive charge carried by the PIL-CS hydrogel inserting hydrophobic groups into the anionic phosphate groups of the bacterial cell wall through electrostatic interactions, causing the bacteria to lyse and die, and not releasing any antimicrobial substance.

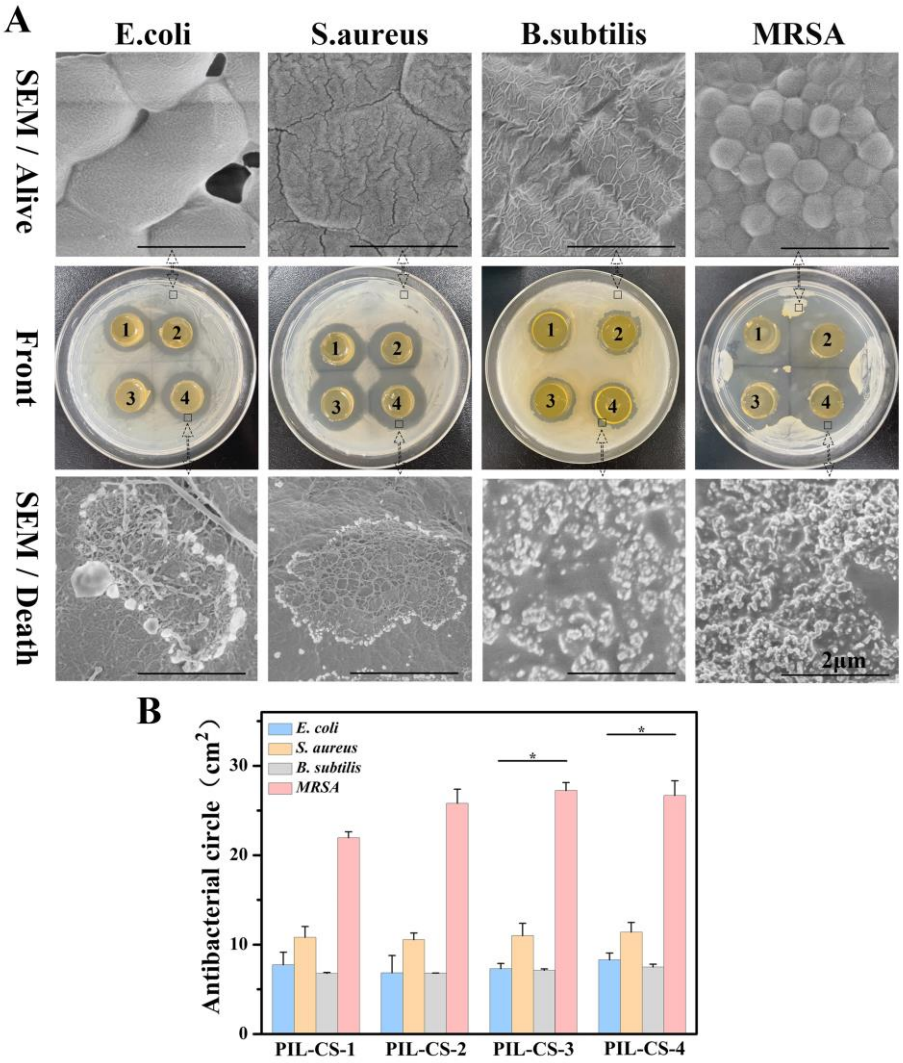

Figure 6. The antibacterial ability of PIL-CS-X (X=1, 2, 3, 4) hydrogels was assessed by disc quorum. A) Photographs of the circle of bacteria inhibition after 24 h co-cultivation of PIL-CS hydrogel with E. coli, S. aureus, Bacillus subtilis and MRSA. Numbers 1- 4 represent PIL-CS-1, PIL-CS-2, PIL-CS-3 and PIL-CS-4, respectively. scale bar is 2 μm; B) The fungicidal activity of the sample surfaces against *E. coli*, *S. aureus*, *Bacillus subtilis* and MRSA was evaluated by the inhibition circle area (data are depicted as mean ± SD, *p < 0.05, n = 3).

Colony formation counts were also employed to feature the antimicrobial property of PIL-CS hydrogels. As shown in **Figure S10(A – D)**, PIL-CS-X (X=1, 2, 3 and 4) with different IL-CHO contents showed antibacterial activity against *E. coli*, *S. aureus*, *B. subtilis* and MRSA. It is noteworthy that almost 98% of bacteria were killed with PIL-CS-4 hydrogel after co-incubation for 24 h. In addition, PIL-CS-3 hydrogel inhibited about 90% of *E. coli*, *S. aureus* and *B. subtilis* growth and inhibited about 95% of MRSA growth (**Figure S10E**).

2.6 *In vitro* cytocompatibility/blood compatibility

To assess the biocompatibility of PIL-CS hydrogels, the material was co-cultured with L929 cells and its cellular activity was measured daily. Double staining of L929 cells after 24 and 48 h of coculture with Calcein-AM/PI to distinguish live cells from dead cells revealed that few red dead cells were observed after staining (**Figure 7A**). CCK-8 results showed that the cell viability of the L929 cell samples remained around 98% after being co-cultured for 3 days, indicating that the PIL-CS hydrogel has good cytocompatibility (**Figure 7B**). The experiments also show that the 3D porous structure of PIL-CS hydrogel has a similar structure to ECM in tissues, which could synergize good cytocompatibility and promote cell growth and tissue repair.[34] In addition, excellent blood compatibility is essential for medical materials.

The effect of thrombotic reactions of PIL-CS hydrogels in blood contact was evaluated by whole blood.[2] As shown in **Figure 7C**, some blood cells and clots were attached to the commercial excipient 3M Tegaderm, while our four PIL-CS hydrogels were found without blood clotting. Subsequently, the hemolysis rate (HR) of PIL-CS hydrogels was quantitatively assessed. The hemolysis rate of medical materials is usually required to be less than 5%. The hemolysis rates of all four PIL-CS hydrogels were found to meet the

requirements (**Figure 7D**). The above results indicate that PIL-CS hydrogel has good biocompatibility and is suitable as a medical dressing to promote wound healing.

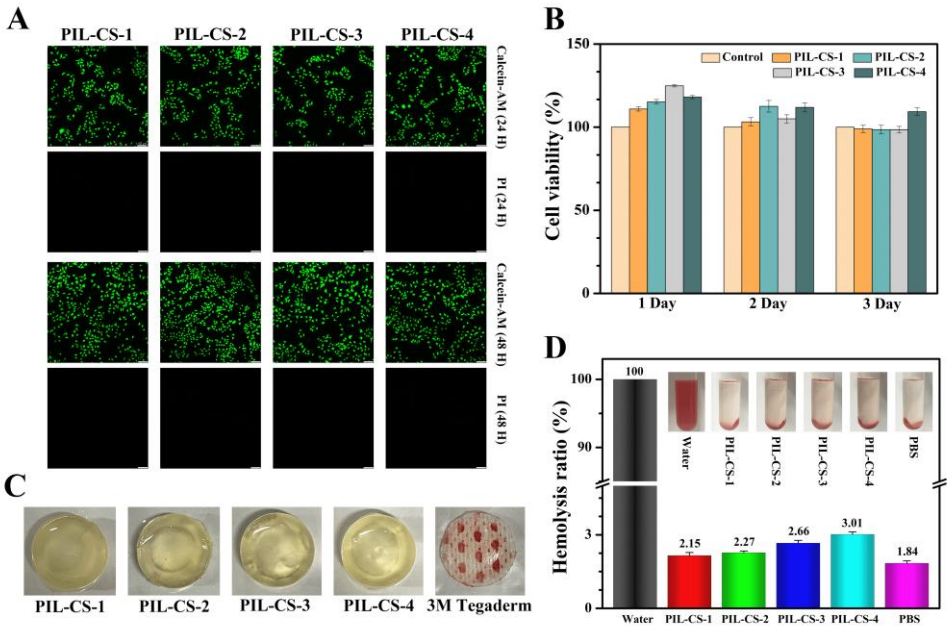

Figure 7. Evaluation of the biocompatibility of PIL-CS-X (X=1, 2, 3, 4) hydrogels. A) Live (green)/dead (red) stained pictures of L929 cells, scale bar is 100 μm; B) Quantitative statistics of L929 cell viability as determined by CCK-8 (data are depicted as mean ± SD, *p < 0.05, **p < 0.01, n = 3); C) Photographs of blood cell adhesion; D) Representative display images and quantitative statistics of the hemolysis ratio of PIL-CS hydrogels (data are depicted as mean ± SD, *p < 0.05, **p < 0.01, n = 3).

2.7 Assessment of L929 cell migration by NIR fluorescent hydrogels

The influence of four PIL-CS hydrogels on cell migration was assessed by in vitro cell scratch assay. As shown in **Figure S11**, the scratch distance by co-culture of L929 cells with hydrogel was smaller than that of the control after 12 h and it was found to be more obvious after being cultured for 24 h. The finding showed that PIL-CS hydrogel could significantly

promote cell migration and proliferation. It is reported that dressings that promote cell migration in vitro can accelerate wound healing in living organisms.[35] Therefore, PIL-CS hydrogel may promote wound healing.

2.8 Adhesion and hemostatic capacity

The adhesion ability of PIL-CS hydrogels onto PP, PE, metal, rubber and glass was investigated. As shown in **Figure S12**, PIL-CS hydrogels can easily adhere to various substrate surfaces in air or water that can resist the interaction between the substrate and the hydrogel.[36] In addition, **support video S6** demonstrates the adhesion of the PIL-CS hydrogel to the skin under the water flow. PIL-CS hydrogels were used in vitro and in vivo hemostasis experiments in mice to evaluate their hemostatic ability. From the hemostasis models of the liver (**Figure S13A**) and severed tail (**Figure S13B**), it was found that the bleeding volume of mice hemostatic with PIL-CS hydrogel was 104.25 and 65.10 mg, while for the blank group was 7 and 17 times higher. The results may support that PIL-CS hydrogels have the excellent hemostatic ability in vitro and in vivo.

2.9 Real-time pH monitoring and imaging in vivo

2.9.1 NIR fluorescence imaging in live cells

The application of CyO and PIL-CS hydrogel in monitoring pH changes in live cells was investigated. The fluorescence intensity of live cells at various pH conditions (4.5, 5.5, 6.0, 6.5, 7.0 and 7.4) was measured after incubating CyO and PIL-CS hydrogel with L929 cells. The live images were also taken with confocal microscopy. As shown in **Figure 8**, the fluorescence intensity of L929 cells was decreased for both CyO and PIL-CS hydrogel when

the pH increased from 4.5 to 7.4. The results support that the hydrogel can monitor real-time pH changes in live cells.

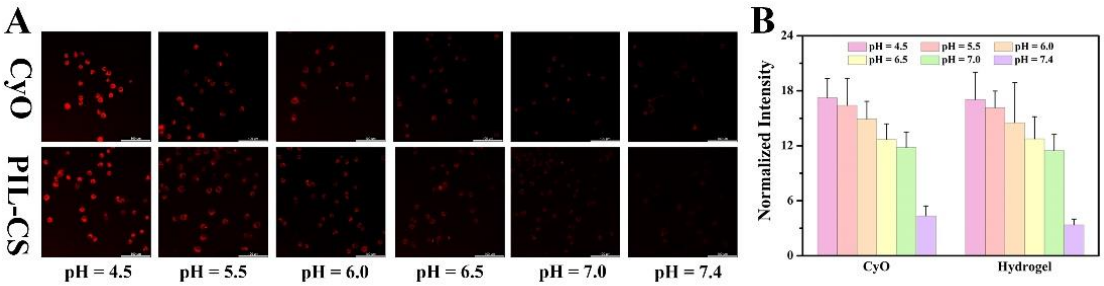

Figure 8. NIR fluorescence imaging live cells. A) Fluorescent pictures showing L929 cells cultivated with CyO (10 μM) and DMEM at different pH levels (4.5, 5.5, 6.0, 6.5, 7.0 and 7.4); B) Quantitative analysis. λex = 660 nm, λem = 780 - 880 nm, scale bar is 100 μm (data are depicted as mean ± SD, *p < 0.05, **p < 0.01, n = 3).

2.9.2 Real-time in vivo visualizing and monitoring of wound pH in a mouse model

The light from the near-infrared (NIR) region (650 - 900 nm) has high penetration ability, induces less background autofluorescence disturbance during bioimaging and also causes low photodamage to biological tissues.[37] Therefore, CyO integrated with hydrogels is ideally suited for real-time imaging and monitoring of chronic wounds such as those of diabetic foot. A wound was surgically created on the back of KM mice as a model for investigation. As shown in **Figure 9A**, the microenvironment pH at the wound was adjusted from 7.4 to 4.5 and then increased to 7.4. The fluorescence intensity of the hydrogel was found increased and then weakened correspondingly to the pH changes. A clear trend has shown in **Figure 9B** is observed from the quantitative analysis of the fluorescence intensity. It is well known that acute wounds usually have a pH value between 4-6. When the pH rises, the risk of wound infection also increases. Moreover, chronic wounds are usually at alkaline pH.[6] Therefore,

this novel NIR real-time imaging system offers a convenient tool for both acute and chronic wounds care.

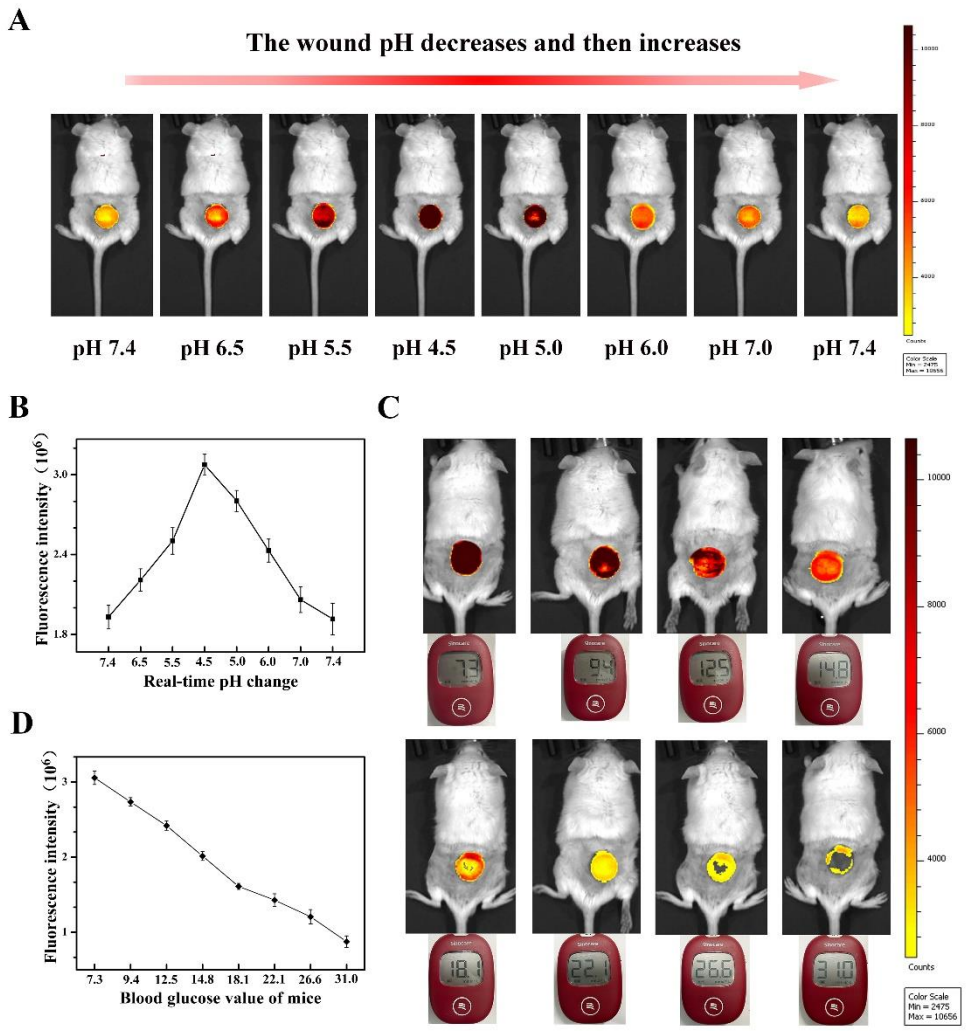

Figure 9. A) NIR fluorescence imaging mouse wounds at different pH levels (7.4, 6.5, 5.5, 4.5, 5.0, 6.0, 7.0 and 7.4); B) Relationship between fluorescence intensities and pH values (data are depicted as mean ± SD, *p < 0.05, **p < 0.01, n = 3); C) Fluorescence imaging of the mouse wound microenvironment in diabetic mice with different blood glucose values (7.3, 9.4, 12.5, 14.8, 18.1, 22.1, 26.6 and 31.0 mmol L^{-1}); D) Quantitative profiling of the

relationship between fluorescence intensity and blood glucose. λex = 640 nm, λ_{em} = 780-880 nm (data are depicted as mean ± SD, *p < 0.05, **p < 0.01, n = 3).

Diabetic wounds usually have an abnormal pH microenvironment and a high glucose level. These adverse factors impede the healing of diabetic skin wounds.[38] We thus investigated the relationship between fluorescence imaging of pH response and the corresponding glucose level at the diabetic wound site in a mouse model with PIL-CS hydrogel. As shown in **Figure 9C**, the hydrogel dressing emitted a stronger signal in the mice with lower blood glucose levels. On the contrary, a much weaker fluorescence signal was generally observed in the mice with higher blood glucose levels. The quantitative analysis of the fluorescence intensity of the PIL-CS hydrogel was shown in **Figure 9D**. The fluorescence signal at the wound decreases as the blood glucose level increases, which may give a sign that the wound could be a diabetic wound because chronic wounds usually have an alkaline pH microenvironment at the wound site.

2.10 Evaluation of wound healing in diabetic mice

The capacity of PIL-CS hydrogel to promote diabetic wound healing was assessed in a diabetic mouse model. A full skin defect model on the back of diabetic mice was established for experiments. PBS and a commercial plugging material, 3M Tedagerm, were used as blank and control groups, respectively. In addition, when PIL-CS hydrogel was injected into the defective skin of diabetic mice, the hydrogel was completely covered and conformed to the area and shape of the wound. As shown in **Figure 10A**, the wound healing rate of the experimental mice was greater than that of the blank and control group at days 3, 7, 12, 14 and 16. Notably, the diabetic wound in the experimental group treated with PIL-CS hydrogel

had a healing rate of almost 100% by day 16 of treatment. This may be attributed to the antimicrobial, antioxidant and sustained drug release capabilities of PIL-CS hydrogel, as well as its ability to closely adhere to the wound site and absorb excess wound exudate. All these properties may facilitate diabetic wound healing. The quantitative analysis of the wound healing rate in the experimental mice was shown in **Figure 10B**. The above results demonstrate that PIL-CS hydrogel promotes diabetic wound healing.

To investigate further the regenerated tissues of diabetic mice, hematoxylin and eosin (H&E) and Masson trichrome staining methods were used to stain the regenerated tissues of diabetic mice after 16 days of PIL-CS hydrogel treatment. **Figure 10C** demonstrates the H&E staining, showing the healing of the wound site with a larger area of immature tissue of approximately 2700 μm in diameter in the blank group and a slightly smaller area in the control group than the blank group. Nonetheless, the regenerated tissue in the four PIL-CS hydrogels group shows the best healing effect. The regenerated tissue cells in the hydrogel group of mice were found significantly and more orderly arranged and had more angiogenesis. The results further demonstrate that PIL-CS hydrogel may promote diabetic wound healing. Re-epithelialization thickness is likewise another important indicator of wound healing. **Figure 10D** shows Masson-stained images of regenerated tissue sites in diabetic mice after 16 days of treatment. The epidermal layer after PIL-CS hydrogel treatment (41.2-61.7 μm) was much significantly larger than that of PBS (14.7 μm) and 3M Tedagerm groups (23.5 μm). Therefore, these results most likely support that PIL-CS hydrogel may effectively promote diabetic wound healing.

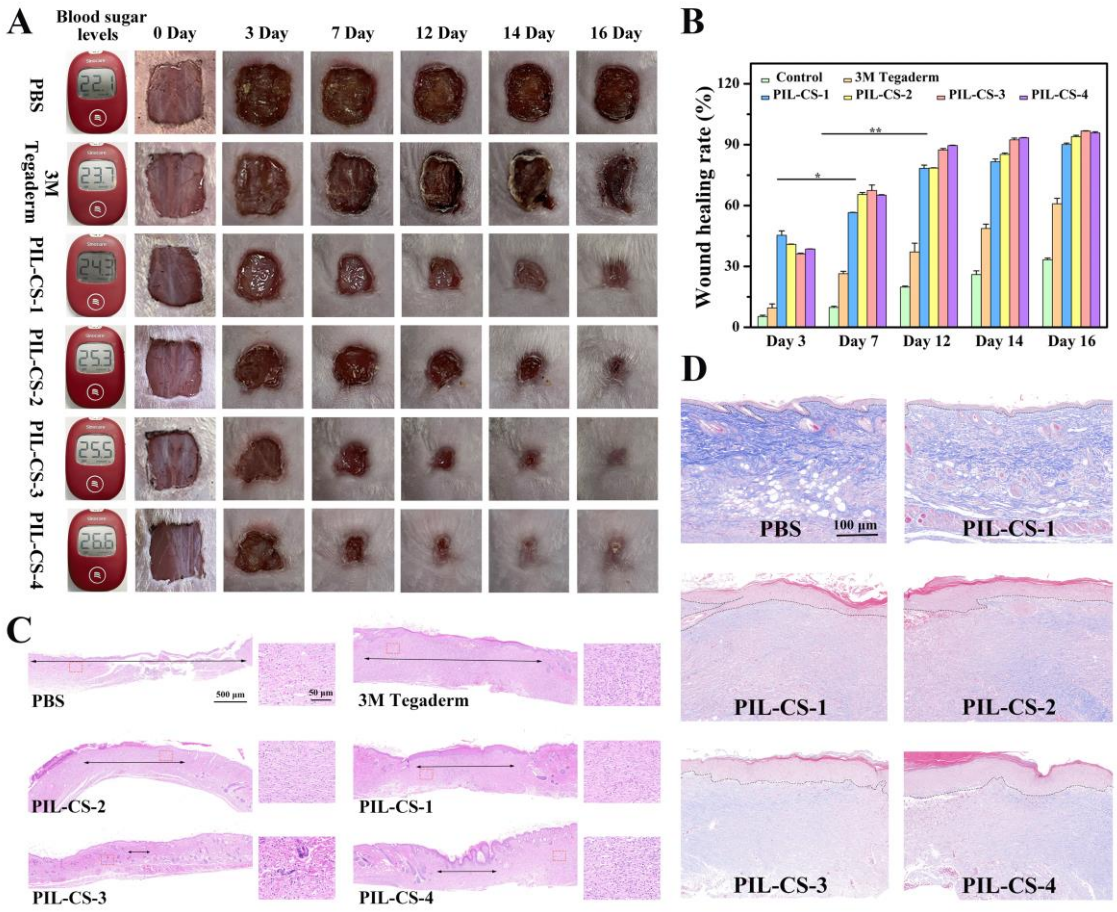

Figure 10. Healing effect of PBS, 3M Tegaderm and PIL-CS-X (X=1, 2, 3, 4) hydrogels in diabetic mice. A) Representative pictures of wounds on days 0, 3, 7, 12, 14 and 16; B) Wound repair rate (data are depicted as mean ± SD, *p < 0.05, **p < 0.01, n = 3); C) H&E staining of wound regeneration tissues, black double arrows indicate the cross-sectional length of immature tissue, scale bar is 500 μm; D) Masson's Trichrome staining of the wound regeneration tissue; The epidermal layer border is highlighted by a black dashed line, scale bar is 100 μm.

To investigate why PIL-CS hydrogels improve wound healing efficiency at the molecular level, immunofluorescence staining of regenerated skin was performed to assess

the expression levels of reactive oxygen species (ROS), tumor necrosis factor (TNF-α) and vascular endothelial growth factor (VEGF). All these factors are the essential cytokines that directly respond to the state of wound healing. In diabetic wounds, excess ROS are produced from immune cells, leading to apoptosis and DNA aggregation in fibroblasts and causing cellular dysfunction and prolonged scarring or failure in wound healing.[29] TNF-α, as a pro-inflammatory factor produced mainly from neutrophils, is an important marker of wound inflammation.[39] Trace amounts of ROS and TNF-α are known to facilitate wound healing. However, when they are produced in excess, they damage wound tissue regeneration.[40] In contrast, VEGF, a growth factor that promotes angiogenesis, actively regulates multiple pathways that promote wound healing.[41] As shown in **Figure 11**, 16 days after diabetic wound healing, the hydrogel dressing significantly reduced the production of ROS (34-43%) at the wound site compared to the 3M Tegaderm commercial film. This result suggests that PIL-CS hydrogel has a good ROS-clearing ability to facilitate the evolution of diabetic wounds from the inflammatory phase to the value-added phase. Notably, PIL-CS hydrogel showed the down-regulation of TNF-α (5-9%) and the up-regulation of VEGF (3-4%) in the promotion of diabetic wound healing. These results confirm that the modulation of ROS, TNF-α and VEGF expression by the treatment of diabetic wounds by PIL-CS hydrogel has a synergistic effect on reducing wound inflammation and promoting tissue formation. It is thereby accelerating diabetic wound healing.

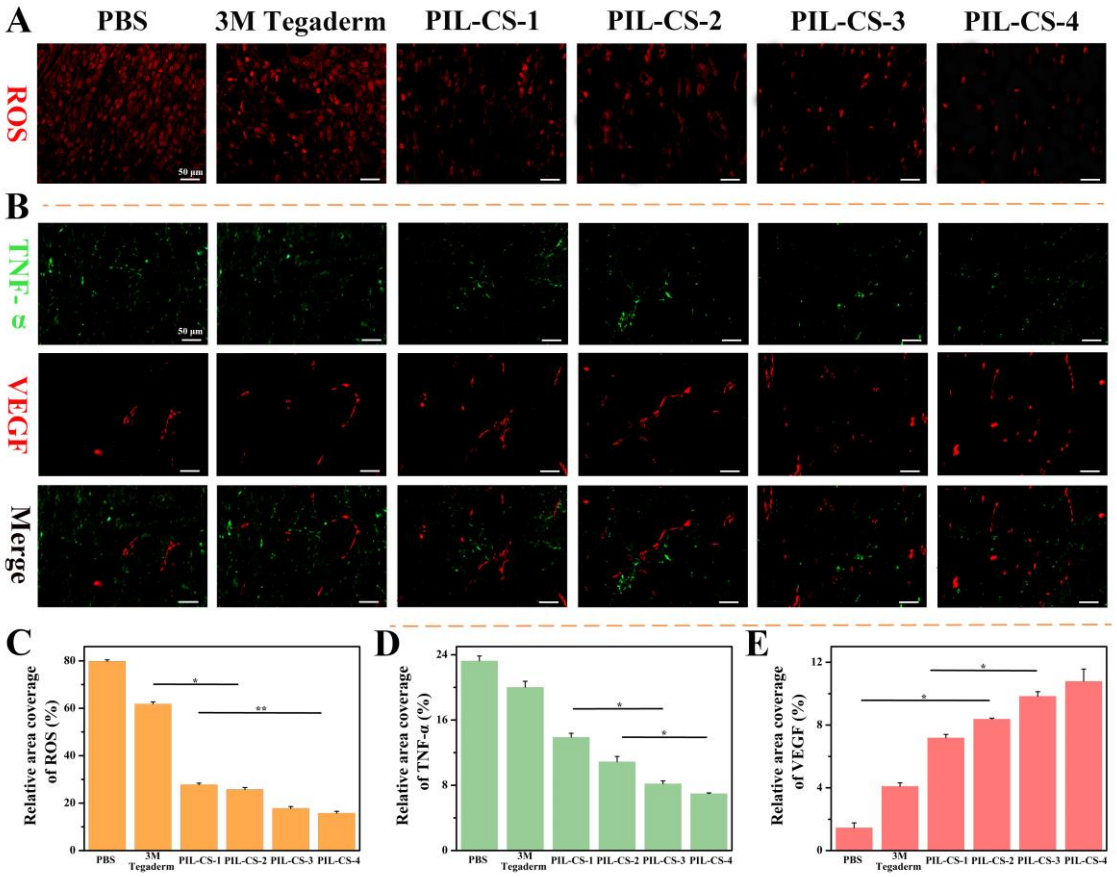

Figure 11. Immunofluorescence staining of recycled skin tissue after being treated with PBS, 3M film dressing and PIL-CS-X (X=1, 2, 3, 4) hydrogels. A) Photograph of the immunofluorescent stained tissue on day 16 after injury, the ROS is smeared in red, the scale bar is 50 μm; B) Photographs of immunofluorescence stained tissues after day 16 of wound processing, TNF-α and VEGF were stained green and red, respectively, the scale bar is 50 μm; The relative percentage of area covered by ROS (C), TNF-α (D) and VEGF (E) in the regenerating wound tissue (data are depicted as mean ± SD, *$p < 0.05$, **$p < 0.01$, $n = 3$).

2.10 Systemic toxicity evaluation

We demonstrated that the PIL-CS hydrogel was applied to the wounds of diabetic mice for up to 16 days and no abnormality in the health and mobility of the mice were observed. The H&E staining of the major organs (heart, liver, spleen, lungs and kidneys) of treated mice were also performed. The results show no abnormal lesions and indicate that the PIL-CS hydrogel may be able to monitor and promote diabetic wound healing, and also causes no damage to major organs (**Figure S14**). The results support that PIL-CS hydrogel has good in vivo biocompatibility and biosafety for practical applications.

3. Conclusions

In conclusion, we developed a multifunctional NIR fluorescent hydrogel with injectable, antibacterial, antioxidant and real-time monitoring properties for promoting diabetic wound healing. The grafted NIR fluorescent probe CyO onto the modified CS backbone allowed PIL-CS hydrogels to obtain pH-responsive, highly reversible and real-time monitor functions. The fluorescence intensity of hydrogels assessed by NIR in vivo imaging instrument for direct response to pH and indirect response to blood glucose changes at the wounds is able to prevent irregular wound infections and provide aids for diabetic wound care. More importantly, PIL-CS hydrogel has long-lasting drug release, antioxidant and ROS scavenging properties that help reduce the production of inflammation and high oxidative contingency at the wound site. The good skin hemostasis and adhesion, electrical conductivity, antimicrobial properties and biocompatibility of the hydrogel synergistically improve the efficiency of diabetic wound healing. Good mechanical properties, frost protection and water resistance also enhance the usefulness of PIL-CS hydrogel. These merits of the material show great potential for preparing wearable real-time detection devices in the future. Therefore, PIL-CS hydrogel is an excellent wound dressing for the diagnosis and treatment of diabetic wounds.

4. Experimental Section

Experimental details are provided in the supporting information.

Supporting Information

Supporting Information is available from the Wiley Online Library or from the author.

Acknowledgements

This project was supported by the National Natural Science Foundation of China (Nos. 22074160, 21874157, 22004133, 21675175), Fundamental Research Fund for the Central University of South-Central Minzu University (No. CZZ22003), Health and Medical Research Fund, Hong Kong SAR (Project No. 19200231 and 22210412), Hong Kong Polytechnic University, Startup Research Fund (P0043754) and Chongqing Natural Science Foundation of China (cstc2021jcyj-msxmX0670). All animal experiments were performed in accordance with the Guide for the Care and Use of Laboratory Animals of the South-Central Minzu University and were approved by the Institutional Ethics Committee of South-Central Minzu University (No. 2020-scuec-045). The operator has passed the professional technical examination for laboratory animals (No. TY20201031). All animals in the experiments were in good condition according to the requirements of the National Laboratory Animal Law (China).

Conflict of Interest

The authors declare no conflict of interest.

Data Availability Statement

The data that supports the findings of this study are available in the supplementary material of this article.

References

[1] K. Zheng, Y. Tong, S. Zhang, R. He, L. Xiao, Z. Iqbal, Y. Zhang, J. Gao, L. Zhang, L. Jiang, Y. Li, *Adv. Funct. Mater.* **2021**, *31*, 2102599.

[2] Y. Zhu, J. Zhang, J. Song, J. Yang, Z. Du, W. Zhao, H. Guo, C. Wen, Q. Li, X. Sui, L. Zhang, *Adv. Funct. Mater.* **2019**, *30*, 1905493.

[3] Z. Wang, L. Liu, W. Bu, M. Zheng, N. Jin, K. Zhang, X. Xu, D. Zhou, B. Yang, H. Sun, *Adv. Funct. Mater.* **2020**, *30*, 2004886.

[4] Y. Jia, X. Zhang, W. Yang, C. Lin, B. Tao, Z. Deng, P. Gao, Y. Yang, K. Cai, *J Mater Chem B* **2022**, *10*, 2875-2888.

[5] W. Cao, S. Peng, Y. Yao, J. Xie, S. Li, C. Tu, C. Gao, *Acta Biomater* **2022**, *152*, 60-73.

[6] L. Wang, M. Zhou, T. Xu, X. Zhang, *Chem. Eng. J.* **2022**, *433*, 134625.

[7] X. Zhao, Y. Liang, Y. Huang, J. He, Y. Han, B. Guo, *Adv. Funct. Mater.* **2020**, *30*, 1910748.

[8] M. Sharifuzzaman, A. Chhetry, M. A. Zahed, S. H. Yoon, C. I. Park, S. Zhang, S. Chandra Barman, S. Sharma, H. Yoon, J. Y. Park, *Biosens Bioelectron* **2020**, *169*, 112637.

[9] Y. Liang, M. Li, Y. Yang, L. Qiao, H. Xu, B. Guo, *ACS Nano* **2022**, *16*, 3194-3207.

[10] W. Chen, S. Xu, J. J. Day, D. Wang, M. Xian, *Angew Chem Int Ed Engl* **2017**, *56*, 16611-16615.

[11] S. Bernhard, M. W. Tibbitt, *Adv Drug Deliv Rev* **2021**, *171*, 240-256.

[12] Y. Liang, X. Zhao, P. X. Ma, B. Guo, Y. Du, X. Han, *J Colloid Interface Sci* **2019**, *536*, 224-234.

[13] M. Ma, Y. Zhong, X. Jiang, *Carbohydr Polym* **2020**, *236*, 116096.

[14] B. Zhang, Y. Qin, L. Yang, Y. Wu, N. Chen, M. Li, Y. Li, H. Wan, D. Fu, R. Luo, L. Yuan, Y. Wang, *ACS Nano* **2022**, *16*, 6585-6597.

[15] Y. Lu, H. Li, J. Wang, M. Yao, Y. Peng, T. Liu, Z. Li, G. Luo, J. Deng, *Adv. Funct. Mater.* **2021**, *31*, 2105749.

[16] S. Li, S. Dong, W. Xu, S. Tu, L. Yan, C. Zhao, J. Ding, X. Chen, *Adv Sci (Weinh)* **2018**, *5*, 1700527.

[17] H. Xu, Y. Xie, E. Zhu, Y. Liu, Z. Shi, C. Xiong, Q. Yang, *J. Mater. Chem. A* **2020**, *8*, 6311-63186311.

[18] Z. Wang, Y. Cong, J. Fu, *J Mater Chem B* **2020**, *8*, 3437-3459.

[19] Z. P. She, Y. Tian, Y. S. Xia, J. Jie, Y. Li, C. Y. Li, *Dyes Pigments* **2020**, *179*, 108402.

[20] Y. Wang, X. Yang, X. Chen, X. Wang, Y. Wang, H. Wang, Z. Chen, D. Cao, L. Yu, J. Ding, *Adv. Funct. Mater.* **2022**, *32*, 2206554.

[21] Y. Zhou, X. Fei, J. Tian, L. Xu, Y. Li, *J. Colloid Interface Sci.* **2022**, *606*, 192-203192.

[22] P. Liu, K. Jin, Y. Zong, M. He, C. Lu, H. Li, Y. Wang, C. Li, *Biomater Sci* **2022**, *10*, 1795-1802.

[23] L. Fan, C. Xiao, P. Guan, Y. Zou, H. Wen, C. Liu, Y. Luo, G. Tan, Q. Wang, Y. Li, P. Yu, L. Zhou, C. Ning, *Adv Healthc Mater* **2022**, *11*, e2101556.

[24] X. Zhao, B. Guo, H. Wu, Y. Liang, P. X. Ma, *Nat Commun* **2018**, *9*, 2784.

[25] Y. Zhao, Z. Li, S. Song, K. Yang, H. Liu, Z. Yang, J. Wang, B. Yang, Q. Lin, *Adv. Funct. Mater.* **2019**, *29*, 1901474.

[26] F. Luo, A. Das, J. Chen, P. Wu, X. Li, Z. Fang, *Cardiovasc Diabetol* **2019**, *18*, 54.

[27] Y. Liang, J. He, B. Guo, *ACS Nano* **2021**, *15*, 12687-12722.

[28] X. Yan, W. W. Fang, J. Xue, T. C. Sun, L. Dong, Z. Zha, H. Qian, Y. H. Song, M. Zhang, X. Gong, Y. Lu, T. He, *ACS Nano* **2019**, *13*, 10074-10084.

[29] Z. Xu, S. Han, Z. Gu, J. Wu, *Adv Healthc Mater* **2020**, *9*, e1901502.

[30] S. Roy, J. W. Rhim, *Food Hydrocolloid.* **2019**, *94*, 391-398391.

[31] J. Qu, X. Zhao, Y. Liang, Y. Xu, P. X. Ma, B. Guo, *Chem. Eng. J.* **2019**, *362*, 548-560548.

[32] Y. Wu, Y. Wang, L. Long, C. Hu, Q. Kong, Y. Wang, *J Control Release* **2022**, *341*, 147-165.

[33] H. Fang, J. Wang, L. Li, L. Xu, Y. Wu, Y. Wang, X. Fei, J. Tian, Y. Li, *Chem. Eng. J.* **2019**, *365*, 153-164153.

[34] S. Liarte, A. Bernabe Garcia, F. J. Nicolas, *Cells* **2020**, *9*, 9010255.

[35] Y. Yuan, S. Shen, D. Fan, *Biomaterials* **2021**, *276*, 120838.

[36] L. Rong, X. Xie, W. Yuan, Y. Fu, *ACS Appl. Mater. Interfaces* **2022**, *14*, 29273-29283.

[37] F. Yang, Q. Zhang, S. Huang, D. Ma, *J Mater Chem B* **2020**, *8*, 7856-7879.

[38] S. Wang, H. Zheng, L. Zhou, F. Cheng, Z. Liu, H. Zhang, L. Wang, Q. Zhang, *Nano Lett* **2020**, *20*, 5149-5158.

[39] A. Singh, R. Bhattacharya, A. Shakeel, A. K. Sharma, S. Jeevanandham, A. Kumar, S. Chattopadhyay, H. B. Bohidar, S. Ghosh, S. Chakrabarti, S. K. Rajput, M. Mukherjee, *Mater. Horiz.* **2019**, *6*, 274-284274.

[40] J. Qian, L. Ji, W. Xu, G. Hou, J. Wang, Y. Wang, T. Wang, *ACS Appl. Mater. Interfaces* **2022**, *14*, 16018-16031.

[41] S. Huang, H. Liu, K. Liao, Q. Hu, R. Guo, K. Deng, *ACS Appl. Mater. Interfaces* **2020**, *12*, 28952-28964.

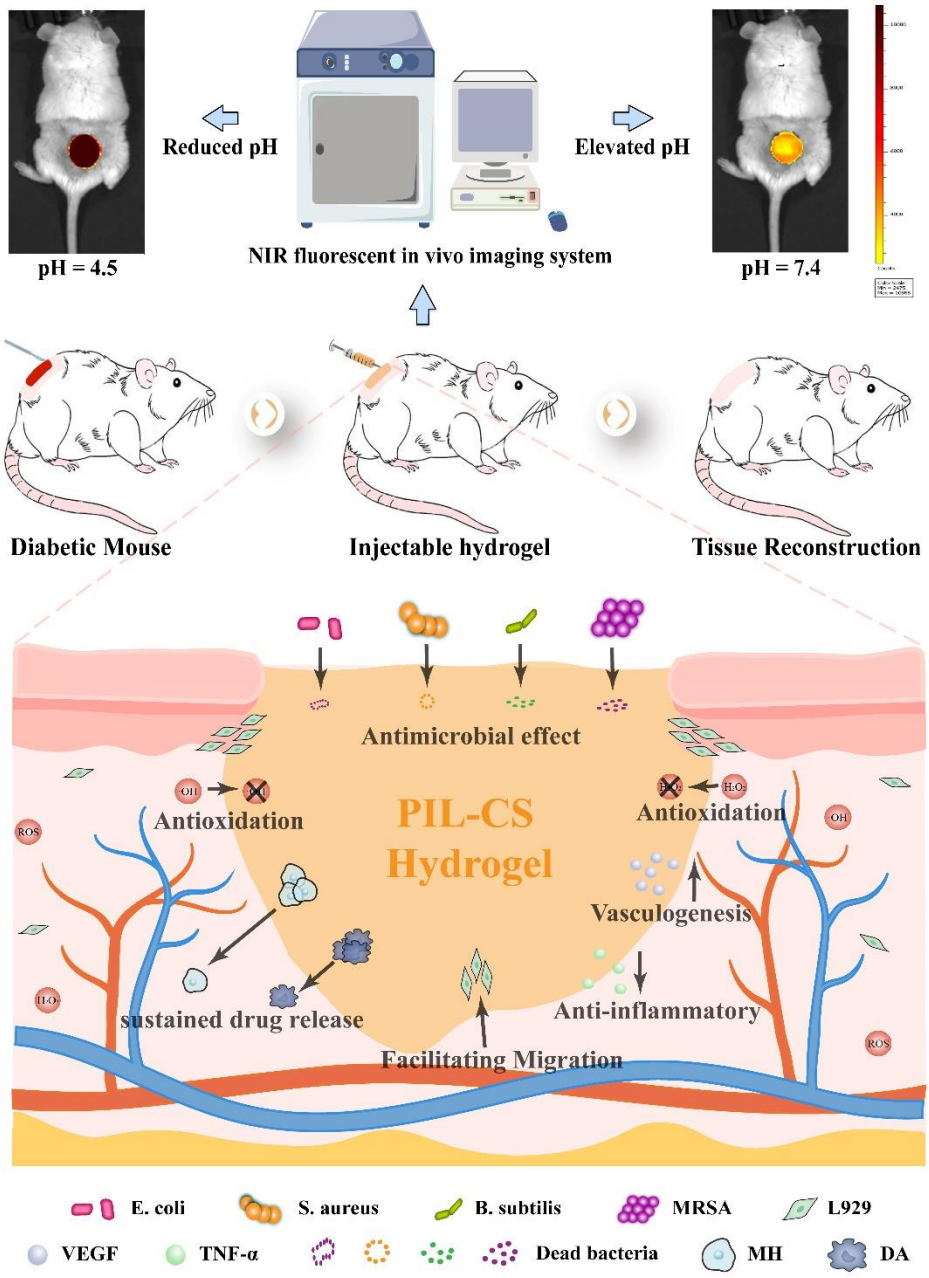

Multi-functional chitosan hydrogel based on polymerized ionic liquid and a NIR fluorescent probe was synthesized and used as a dressing for real-time monitoring wound pH through *in vivo* NIR fluorescent imaging and promoting diabetic wound healing through

effective antimicrobial properties, antioxidant properties, sustained drug release, anti-inflammatory, and the promotion of cell migration and angiogenesis.